Published in final edited form as:
Plast Reconstr Surg. 2011 November ; 128(5): 438e–450e. doi:10.1097/PRS.0b013e31822b7352.

Wound Contraction is Attenuated by Fasudil Inhibition of Rho-Kinase

Jennifer E. Bond, PhD[1,*], **George Kokosis, MD**[1,*], **Licheng Ren, MD**[1], **M. Angelica Selim, MD**[2], **Andrew Bergeron, BS**[1], and **Howard Levinson, MD**[1,2]

[1]Division of Plastic and Reconstructive Surgery, Department of Surgery, Duke University Medical Center, Durham NC 27710

[2]Department of Pathology, Duke University Medical Center, Durham NC 27710

Abstract

Background—Dermal scarring and scar contracture result in restriction of movement. There are no effective drugs to prevent scarring. RhoA and Rho Associated kinase (ROCK) have emerged as regulators of fibrosis and contracture. Fasudil, a ROCK inhibitor, has been demonstrated to have anti-fibrotic effects in models of liver, renal and cardiac fibrosis. The role of fasudil in preventing dermal scarring and contractures has not been studied. We use a rat model of dermal wound healing to assess the effects of fasudil for preventing scarring.

Methods—Human scar tissue and surrounding normal skin were immunostained for RhoA and ROCK. Full-thickness wounds were created on Wistar-han rats and fasudil (30mg/kg/d) or saline were continuously delivered subcutaneously. Wound contraction was measured by gravitational planimetry. After 21d, tissue was harvested for Masson's trichrome, H&E, Ki-67 and CD-31 staining. Fibroblast populated collagen lattices were utilized to assess the mechanistic effects of fasudil on contractility. Myofibroblast formation was assessed in the presence of fasudil.

Results—Human scar tissue in the remodeling phase of repair showed increased expression of RhoA and ROCK in scar tissue compared to surrounding normal tissue. Fasudil inhibited wound contraction as compared to controls. H&E and Masson's were similar between groups. Fasudil did not alter angiogenesis or proliferation. Fasudil inhibited fibroblast contractility, and myofibroblast formation *in vitro*.

Conclusions—There is growing evidence that RhoA/ROCK pathway plays an important role in wound healing and scar contracture. We present data that inhibition of ROCK hinders fibroblast contractility and may be beneficial in preventing scar contracture.

INTRODUCTION

Dermal scars are disfiguring and disrupt daily activities. There are no effective drugs to prevent scarring and revisional surgery is the main treatment. Scar contractures are thought

Corresponding Author Howard Levinson, MD, FACS, Assistant Professor Division of Plastic and Reconstructive Surgery, Assistant Professor Pathology, Departments of Surgery and Pathology, DUMC 3181, Durham, NC 27710, P (919) 684-8661, F (919) 681-7340, howard.levinson@duke.edu.
*Co-first author.

Financial Disclosure The authors do not have conflicts of interest to report.

Chemicals Used The chemical used was fasudil (LC Laboratories, Woburn, MA).

to develop from extracellular matrix remodeling by highly contractile myofibroblasts.[1, 2] Cell contractility is stimulated by the pro-contractile small GTP-ase RhoA, which phosphorylates and activates downstream kinase, Rho-associated coiled coil-containing protein kinase (ROCK).[1, 3, 4]

ROCK promotes actomyosin mediated contractile force generation through phosphorylation of LIM kinase -1 and -2, myosin regulatory light chain, and myosin regulatory light chain phosphatase.[5] ROCK also activates the transcription factors, myocardin related transcriptional factor and serum response factor, which in turn up-regulate expression of alpha smooth muscle actin.[6] ROCK is an important regulator of cytoskeleton function, mediating stress fiber and focal adhesion formation, cell contractility, adhesion, membrane ruffling, and motility.[4] ROCK is also an important regulator of proliferation, differentiation, and apoptosis.[4, 7] ROCK is inhibited by the FDA approved drug, fasudil (HA-1077).

Fasudil is a selective ROCK inhibitor that targets the ATP dependent kinase domains of ROCK.[8, 9] Fasudil has been demonstrated to have anti-fibrotic effects in cardiac, hepatic, pulmonary, renal and ocular fibrosis.[10–14] Fasudil has attenuated angiotensin II-induced cardiac hypertrophy and perivascular fibrosis in apolipoprotein E deficient mice.[15] Fasudil has decreased cardiac and renal fibrosis in diabetes mellitus rat models when dosed 100mg/kg/day (18% reduction in collagen III deposition in left ventricle versus 1.6% in controls and 0.95% incidence of renal cortical fibrosis in fasudil treated group versus 7% in controls).[16] Fasudil given in hypertensive rat models with glomerulosclerosis, improved renal function (30–40% decrease in serum creatinine and blood urea nitrogen, 30% decrease in proteinuria) and decreased histological injury.[17, 18] Liver fibrosis in rats induced by carbon tetrachloride was significantly reduced by 10mg/kg/day fasudil, as recorded by aspartate transferase (AST) levels (82±14 IU/L) when compared to controls (593±174 IU/L).[12] Fasudil was found to ameliorate diabetes mellitus induced ocular fibrosis, when injected intravitreally at a concentration of 30μmol/L in rabbit eyes.[19] The role of fasudil in preventing dermal fibrosis has not been investigated. Here we study the expression of RhoA and ROCK in human dermal scar, determine the effects of fasudil on rat excisional dermal wound healing, and determine the effects of ROCK inhibition on primary human dermal fibroblast contractility *in vitro* as a mechanism to explain the *in vivo* findings.

MATERIALS AND METHODS

Cell Culture

Fibroblasts were explanted from human scar tissues excisions (age of scars between 30 – 90d) as approved by the Duke University Medical Center (DUMC) Institutional Review Board. Three human fibroblast cell lines were established from three different patients. In brief, tissues were minced with a scalpel and incubated in collagenase type I with 1% penicillin/streptomycin (Sigma-Aldrich, St. Louis, MO, USA) at 37°C for 4h. The cells were cultured in DMEM with 10% FBS and 1% penicillin/streptomycin. Experiments with primary cell cultures were performed when cells became 80–90% confluent between passages 1–6. Fibroblasts were cultured with 5ng/ml TGF-β for 4d, in the presence of 12.5μM or 25μM fasudil. Following culturing, alpha smooth muscle actin (αSMA) expression was measured using intracellular flow cytometry.[20] Anti-αSMA antibody (mouse monoclonal clone 1A4, Sigma) was incubated for 1h at 4°C following fixation and permeabilization of fibroblasts (BD Cytofix/Cytoperm, BD Biosciences San Diego CA.). Following which fibroblasts were incubated with FITC anti-mouse secondary for 45mins at 4°C. Samples were analyzed on a Guava EasyCyte Plus flow cytometer (Guava Technologies, Hayward, CA, USA). A total of 10,000 cells were analyzed in each sample, and data were collected using CytoSoft Data Acquisition and Analysis Software (Guava

Technologies). Data were analyzed and the geometric mean of the fluorescence intensity for each cell type was calculated using Flowjo version 7.6 (Tree Star Inc., Ashland, OR, USA).

Fibroblast Populated Collagen Lattice (FPCL) Contraction

Cell behavior in FPCL contraction closely mimics what is observed in vivo as focal adhesions formation, ECM remodeling and isotonic contraction observed in FPCL contraction parallels the findings in contracting wounds and scars.[2122] The fabrications of both free-floating FPCLs (FF-FPCL) and stressed FPCLs (S-FPCL) were followed as previously described.[20] A mixture of fibroblasts–collagen–medium containing 1.0×10^5 cells/mL, 1.28mg/mL purified collagen, (Nutragen, Advanced Biomatrix, Fremont, CA, USA) and 10% FBS in DMEM (growth media) was added in 400μl volumes to a 24-well flat bottom tissue culture plate. The plate was placed in a 37°C incubator with 5% CO_2 for 60min to allow the collagen to polymerize, before adding 500μL of growth media or growth media and fasudil (0–100μM). S-FPCL where prepared similar, but with 1.0×10^6 cells/mL and cultured for 24h. Following 24h S-FPCL were released and 500μL of growth media or growth media and fasudil (0 – 50μM) was added. The sizes of lattices were recorded using a digital scanner 18h and 5h after release for FF-FPCL and S-FPCL, respectively. The areas of each lattice were determined and measured using ImageJ (NIH, Bethesda, MD, USA). All conditions were performed in triplicate per experiment, and these experiments were repeated three times.

Rodent Model of Wound Healing

A rat excisional wound model was approved by the Institutional Animal Care and Use Committee of DUMC. Ten to 12 week-old (200–225g) Wistar-han female rats (Charles River. Raleigh, North Carolina) were anesthetized with inhaled 2% isoflurane and their dorsum shaved followed by application of a depilatory agent. A full-thickness excisional wound of $4cm^2$ (2×2cm) was created between the scapular angle of each animal. The wounds were covered with Tegaderm™ (3M, St. Paul Mn.). The rats were randomly divided into two groups of ten rodents per group: (i) vehicle control (saline), and (ii) fasudil-treated rates (30mg/kg/d in saline). Alzet® osmotic mini pumps (model 2ML4, 2.5μl/hr delivery rate , 2ml reservoir, and 28d delivery duration Durect Corp., Cupertino, CA) were filled with saline, or fasudil (LC Laboratories, Woburn, MA.) and then implanted subcutaneously into the flank through a distinct incision, separate from the wound. Fasudil and saline were delivered by the pumps into the subcutaneous tissue. The incisions were closed with interrupted 3-0 nylon sutures. The experiment continued for 21d.

Wound Analysis and Assessment

On days 2, 7, 9, 11, 14, and 21 wound size was measured by gravitational planimetry. Wound area was calculated as a percent of original and remaining wound size: $(\frac{remaining}{orginial}) \times 100$. Animals were weighed and assessed for signs of toxicity.

Histology

On day 21, the animals were euthanized using pentobarbital (250mg/kg intraperitoneal injection). The wounds were excised, including a 5mm margin of normal skin around the edges of the wound, and fixed in 10% formalin. The samples underwent histological processing and stained with hematoxylin and eosin (H&E), and Goldner`s modification of Masson`s trichrome stain. The specimens were analyzed for tissue architecture, epithelial regeneration, inflammation, and collagen deposition. Epithelialization was quantified for each specimen by measuring 5 different epithelium thicknesses at 10X magnification.

Immunohistochemistry

CD-31 immunostaining was used to quantify angiogenesis and Ki-67 to quantify proliferation. Formalin fixed, paraffin-embedded tissue blocks were sectioned at 5–10μm. Appropriate positive and negative controls were performed for each antigen assayed. Slides were counterstained with hematoxylin. The sections were incubated with: rabbit anti-Ki-67 (1:50 dilution. monoclonal, RM-9106-S,Thermo scientific, Fremont, CA), or rabbit anti-mouse CD-31 antibody (1:100 dilution, rabbit anti–CD-31 antibody ab28364, Abcam, Cambridge, MA) overnight at 4°C. Tissue staining was visualized using the avidin biotinylated enzyme complex system (Vectastain Elite ABC, Vector. Burlingame. Ca.) and 3,3'-Diaminobenzidine substrate chromogen solution (Dako, Carpinteria, CA). The number of Ki-67 positive nuclei and CD-31 positive vessels were counted in 5 power fields at 40× and 20× magnification, respectively.

Western Blotting

Detection of alpha smooth muscle actin (αSMA) in rat tissue was measured by western analysis. After 21d, tissue was collected and lysed using RIPA buffer (Sigma Alrdich) and protease inhibitor cocktail (Thermo Scientific. Rockford IL.). 5μg of tissue lysates were separated on 4–12% Bis-Tris gel (Invitrogen, Carlsbad, CA.) After electrophoresis, the separated proteins were transferred to a nitrocellulose membrane (Invitrogen). The membrane was incubated with blocking buffer for 1h and then incubated with the primary antibody (αSMA, clone 1A4. Sigma Aldrich, and β-tubulin, H-235 Abcam) at 4°C overnight. The blots were subsequently incubated with the appropriate secondary antibody in blocking buffer. Proteins were visualized using Odyssey Infrared Imager (Model 9120, Li-Cor, Inc, Lincoln, NE).

Immunohistology of Human Tissue for RhoA, ROCK I and ROCK II

Formalin fixed and paraffin embedded tissues were obtained from DUMC, Department of Pathology repository of tissue specimens in accordance with the DUMC Institutional Review Board. Samples were obtained from re-excisions of previous scars. Selection of specimens was based on the age of the scar so that the scars were either in the remodeling phase of repair, which beings on post-operative day fourteen and can continue for up to two years, or after the remodeling phase of repair. Scar re-excisions ranged from post-operative 14d to 1058d (table 1). A sample section of the tissue was stained by hematoxylin and eosin, and reviewed a under light microscope for the presence of the scar and normal tissue within the section. Samples were selected to match for patient's race, gender, age and scar location. Specimens were equivalent across groups ($p \geq 0.05$) except for gender. There were no clinical reports as to the quality of the scars. Human scar tissue of consecutive sections of 5μm was immunostained for RhoA and ROCK. Sections were incubated for 45min with the rabbit, anti-RhoA (Cell Signaling Technology Danvers MA), rabbit anti-ROCKI, or rabbit anti-ROCK II (Santa Cruz Biotechnology, Santa Cruz. CA.), at 1:100 dilution. Staining was visualized as described above.

Statistical Analysis

Results are expressed as mean ± standard error of mean. Statistical analysis was performed using ANOVA. A value of $p \leq 0.05$ was considered statistically significant.

RESULTS

Expression of RhoA, ROCK I and ROCK II in Human Scar Tissue

Human scar samples with surrounding normal skin were selected for immunohistochemical staining of RhoA, ROCK I, and II (see table 1 for demographics). These aged scars were in

the remodeling phase of repair and thus represented scars that could be treated with the ROCK inhibitor fasudil. Figure 1 illustrates selected representative specimens from 84d scars (remodeling phase) stained for RhoA, ROCK I and II. RhoA, ROCK I and II were located in the vessels and muscle of the follicular sebaceous units of normal skin and scar. RhoA expression was focally expressed in normal skin fibroblasts but markedly increased in scar fibroblasts. ROCK I and II expression were detected to a greater extent in the scar compared to surrounding normal tissue.

Fasudil Inhibition of Wound Contraction

To evaluate if fasudil prevents scar contracture, full thickness excisional dermal wounds were created on the dorsum of rodents and the wounds were allowed to contract closed. Animals were treated with either fasudil or vehicle only, using subcutaneous implanted osmotic pumps to ensure reliable continuous systemic delivery. Wound size was measured by gravitational planimetry, and data is shown in Fig. 2. Fasudil delayed closure as compared to controls ($p \leq 0.05$). The relative wound area in the control group was smaller at all time points. Fasudil was not toxic; there were no wound infections or signs of systemic toxicity as determined by parameters of animal behavior. Animal weights were consistently similar between groups (data not shown).

Histological Evaluation of the Effects of Fasudil

H&E staining was used to evaluate rodent dermal healing. H&E revealed epidermal defect with reactive hyperplasia at the wound edges. The wound showed fibroblastic proliferation with lymphohistocytic infiltrates, the fibroblasts were arranged parallel to the epidermis surface, and rich neo-vascularization was displayed perpendicular to the epidermis. Foreign giant cell reaction was seen at the lateral and deep aspect of the scar. Follicular sebaceous units were normal at the edge of the wound. The degree of epidermal reaction between the untreated and fasudil-treated groups was not significantly different (Fig. 3). Masson's trichrome stain demonstrated collagen around newly formed fibroblasts, there was no difference between the untreated and fasudil-treated groups (Fig. 3).

Wound tissue was stained for Ki-67 to assess cell proliferation (Fig. 3). Nuclear immunoreactivity to Ki-67 antibody had a dark brown granular appearance and the positive nuclei were counted (Fig 3). Tissue from the untreated group showed a Ki-67 proliferating index of 31 ± 5 compared to a proliferating index of 39 ± 5 in the fasudil-treated group. The increase in proliferation in the fasudil-treated group was not significant (p=0.42).

Immunohistological staining of the endothelial marker CD-31 was used to evaluate neo-vascularization after 14d. The number of CD-31 positive vessels were counted per high power field and the endothelial index was calculated (Fig. 3). The CD-31 endothelial index for the untreated group was 91±8 and for the fasudil-treated group was 106±3. The difference in neo-vascularization between groups was not significant (p=0.06).

Fasudil Inhibits FPCL Contraction and Prevents Myofibroblast Formation *in vitro*

To test the mechanism how ROCK inhibition reduces wound contraction, we used the free floating and stressed FPCL *in vitro* assays. In the FPCL assay, fibroblasts are enmeshed in three-dimensional collagen gels which they contract over several hours. Free floating FPCL (FF-FPCL) contraction occurs by fibroblast contractility and stressed FPCL (S-FPCL) contraction occurs by myofibroblast contractility. The processes are akin to how fibroblasts contract scars. Primary human dermal fibroblasts were enmeshed in FF-FPCL and stimulated to contract with 10% FBS. Fasudil significantly inhibited FPCL contraction (Fig. 4). Concentrations of fasudil above 12.5μM were required to significantly inhibit contraction ($p<0.05$). Maximum inhibition of contraction was observed at 50μM of fasudil.

The data demonstrated that fasudil inhibited fibroblast contractility. To determine how fasudil affects myofibroblast contractility, primary human dermal fibroblasts were enmeshed in stressed S-FPCL and stimulated to contract with 10% FBS. Fasudil significantly inhibited S-FPCL contraction (Fig.4). Fasudil prevented myofibroblast contractility. To investigate the effect of fasudil on myofibroblast formation *in vitro*, fibroblasts were stimulated with TGF-β to differentiate into myofibroblasts (αSMA actin expression) in the presence or absence of fasudil. Primary dermal fibroblasts incubated with 5ng/ml TGF-β for 4d differentiated into myofibroblasts (Fig. 5). Fasudil (12.5μM and 25μM) significantly decreased the TGF-β stimulated αSMA expression in dermal fibroblasts (Fig. 5). We, then analyzed αSMA expression in untreated and fasudil treated tissue on d21. Fasudil tended to decreased αSMA actin expression but this was not significant.

DISCUSSION

Dermal scarring affects more than 40 million patients annually, ranging from fine lines to severely disfiguring scars and pathologic contractures. Pathologic contractures are the most severe form of scarring. Scars can limit joint motion and there is a need for better preventative therapies. By providing new insights into the molecular mechanisms into signaling pathways of fibroblast activity, more focused treatments can be developed It is possible that the increased expression or activity of signaling kinases could play a role in contracture. One such signaling kinase is ROCK, which is activated by the upstream GTPase, RhoA. Immunohistochemical staining of human scar tissue for RhoA, ROCK I and II showed an increase in expression as compared to normal surrounding tissue. This increase in staining supports the hypothesis that ROCK is likely active in remodeling scars. The mechanism for increased ROCK expression is unknown. Following injury RhoA/ROCK expression could be stimulated due to increased inflammatory response and infection. RhoA/ROCK expression is increased by prostaglandins. [23] and endotoxin both of which are expressed in wound healing and contribute to scarring.[24–26]

The rodent excisional wound model is the most frequently used animal model to study and test anti-scar contracture therapies.[27–30] In this model, a 2×2cm full thickness wound is created on the dorsum of the animal between the scapula. The animal is treated with the therapy and the wound is allowed to heal by second intention. The primary endpoint that is most relevant to scar contracture is the rate of wound contraction, determined by gravitational planimetry. Secondary healing parameters include: (i) epithelialization, (ii) granulation tissue formation, (iii) inflammation, (iv) collagen deposition quantity and pattern, and (v) angiogenesis. In our wound healing studies, fasudil inhibited wound contraction as measured by gravitational planimetry and was non toxic as demonstrated by the presence of grossly normal appearing wound healing, normal behaving animals which consistently gained weight, and similar microscopic appearing wounds. H&E staining, proliferation (Ki-67) and angiogenesis (CD-31) revealed ROCK inhibition did not alter epithelialization, angiogenesis or tissue architecture. Despite reports that fasudil decreases collagen production and deposition, and increases collagenase activity [31, 32], we found that 21d of fasudil treatment did not alter the normal collagen architecture in healing wounds as determined by Masson's trichrome staining. Therefore fasudil likely inhibits wound contraction by different mechanisms.

Our data shows that ROCK inhibition by fasudil prevents FPCL contraction. This suggests that the mechanism by which fasudil prevented wound healing in our *in vivo* model is due to inhibition of fibroblast and myofibroblast contractility. Fibrotic disease is characterized by the failure to halt normal tissue repair and the persistence of myofibroblasts which are highly contractile.[2] Myofibroblast contractility is promoted by several extracellular agonists, such as platelet derived growth factor, TGF-β, sphingosine-1-phosphate, lysophosphatidic

acid, through activation of the small GTPase RhoA and its downstream effector, ROCK.[33–40] Inhibition of ROCK prevents granulation tissue contraction.[38–46] ROCK promotes contractile force generation through sustained phosphorylation of myosin regulatory light chain, and myosin regulatory light chain phosphatase.[47] This prolonged phosphorylation of myosin regulatory light chain, and myosin regulatory light chain phosphatase can incremental scar contractures to form at approximately 1cm per month.[48] Fasudil blocks ROCK-dependent tension generation, preventing dermal fibroblasts from responding to extracellular agonists that normally cause contractility. In addition to fasudil blocking ROCK dependent tension, as an alternative mechanism for the attenuation of wound contraction by fasudil, we evaluated the effect of fasudil on myofibroblast formation. *In vitro* we found that fasudil decreased αSMA expression; however, these finding were not corroborated with our analysis of the *in vivo* tissue. Fasudil did not significantly effect αSMA expression on d21. This discrepancy may reflect limited analyses of time points. We conclude that fasudil inhibition of wound contraction is by blockade of cell contractility and may possibly involve altered myofibroblast formation.

Fasudil has been shown to decreases pulmonary [49], cardiac [50, 51], [15] hepatic, [12], ocular [19], and renal fibrosis.[10] In a rat model of renal fibrosis, fasudil decreased the fibrotic area, histological injury and improved renal function by 30%–50% based on microscopic and macroscopic parameters.[10, 17, 18, 52] Fasudil has not been evaluated for its effect on dermal fibrosis. Our dermal healing study showed that fasudil did not inhibit collagen deposition, cell proliferation or angiogenesis. However, fasudil did decrease contraction *in vivo* and *in vitro*. Since scar contracture is a significantly debilitating component of fibrosis, the data supports the hypothesis that fasudil has anti-fibrotic effects.

The RhoA/Rho-kinase pathway contributes to inflammatory [53] proliferative [7, 54], and remodeling [48] in wound healing. Because of these multiple roles, RhoA and ROCK have emerged as critical regulators of the fibrotic response, including scar contracture formation.[55, 56] Our results provide evidence that ROCK inhibition may be a therapeutic target for preventing scar contractures. It remains to be determined whether ROCK is a critical target for reducing scar contracture. A greater understanding how ROCK is activated and regulated during repair is necessary to develop future therapeutics. Future studies will need to determine dose response curves, dosing routes and the prolonged effects of fasudil on scarring. Beyond the rodent dermal wound healing model, the red-duroc pig and rabbit ear animal models will serve as higher-order assays to validate the efficacy of fasudil in reducing scarring. As drug discovery efforts continue to develop more potent and specific ROCK inhibitors, these drugs could be the first-in-man therapies to treat scarring.

Acknowledgments

Sources of Support: The project was supported by a NIH Mentored Clinical Scientist Award (K08); Grant # GM085562-01, Plastic Surgery Education Foundation Fellowship, supplemental support from the Division of Plastic and Reconstructive Surgery and Departments of Pathology and Surgery at Duke University Medical Center.

References

1. Tomasek JJ, Gabbiani G, Hinz B, et al. Myofibroblasts and mechano-regulation of connective tissue remodelling. Nat Rev Mol Cell Biol. 2002; 3:349–363. [PubMed: 11988769]
2. Gabbiani G. The myofibroblast in wound healing and fibrocontractive diseases. The Journal of Pathology. 2003; 200:500–503. [PubMed: 12845617]
3. Ridley AJ. The GTP-binding protein Rho. The International Journal of Biochemistry & Cell Biology. 1997; 29:1225–1229.
4. Riento K, Ridley AJ. ROCKs: multifunctional kinases in cell behaviour. Nat Rev Mol Cell Biol. 2003; 4:446–456. [PubMed: 12778124]

5. Wettschureck N, Offermanns S. Rho/Rho-kinase mediated signaling in physiology and pathophysiology. Journal of Molecular Medicine. 2002; 80:629–638. [PubMed: 12395147]
6. Small EM, Thatcher JE, Sutherland LB, et al. Myocardin-Related Transcription Factor-A Controls Myofibroblast Activation and Fibrosis in Response to Myocardial Infarction. Circ Res. 2010; 107:294–304. [PubMed: 20558820]
7. Shi J, Wei L. Rho kinase in the regulation of cell death and survival. Archivum Immunologiae et Therapiae Experimentalis. 2007; 55:61–75. [PubMed: 17347801]
8. Asano T, Ikegaki I, Satoh S, et al. Mechanism of action of a novel antivasospasm drug, HA1077. Journal of Pharmacology and Experimental Therapeutics. 1987; 241:1033–1040. [PubMed: 3598899]
9. Shibuya M, Suzuki Y, Sugita K, et al. Effect of AT877 on cerebral vasospasm after aneurysmal subarachnoid hemorrhage. Results of a prospective placebo-controlled double-blind trial. J Neurosurg. 1992; 76:571–577. [PubMed: 1545249]
10. Satoh S, Yamaguchi T, Hitomi A, et al. Fasudil attenuates interstitial fibrosis in rat kidneys with unilateral ureteral obstruction. Eur J Pharmacol. 2002; 455:169–174. [PubMed: 12445583]
11. Tada S, Iwamoto H, Nakamuta M, et al. A selective ROCK inhibitor, Y27632, prevents dimethylnitrosamine-induced hepatic fibrosis in rats. Journal of Hepatology. 2001; 34:529–536. [PubMed: 11394652]
12. Ikeda H, Kume Y, Tejima K, et al. Rho-kinase inhibitor prevents hepatocyte damage in acute liver injury induced by carbon tetrachloride in rats. Am J Physiol Gastrointest Liver Physiol. 2007; 293:G911–G917. [PubMed: 17761835]
13. Nagatoya K, Moriyama T, Kawada N, et al. Y-27632 prevents tubulointerstitial fibrosis in mouse kidneys with unilateral ureteral obstruction. Kidney Int. 2002; 61:1684–1695. [PubMed: 11967018]
14. Takeda Y, Nishikimi T, Akimoto K, et al. Beneficial effects of a combination of Rho-kinase inhibitor and ACE inhibitor on tubulointerstitial fibrosis induced by unilateral ureteral obstruction. Hypertens Res. 2010; 33:965–973. [PubMed: 20664550]
15. Wang YX, da Cunha V, Martin-McNulty B, et al. Inhibition of Rho-kinase by fasudil attenuated angiotensin II-induced cardiac hypertrophy in apolipoprotein E deficient mice. Eur J Pharmacol. 2005; 512:215–222. [PubMed: 15840407]
16. Huntley BK, Ameenuddin S, Chen HH. Differential Anti-Fibrotic Effects of Vardenafil and Fasudil in the Heart and Kidney of Diabetic Rats. Journal of Cardiac Failure. 2010; 16:S31–S31.
17. Kanda T, Wakino S, Hayashi K, et al. Effect of fasudil on Rho-kinase and nephropathy in subtotally nephrectomized spontaneously hypertensive rats. Kidney Int. 2003; 64:2009–2019. [PubMed: 14633123]
18. Nishikimi T, Akimoto K, Wang X, et al. Fasudil, a Rho-kinase inhibitor, attenuates glomerulosclerosis in Dahl salt-sensitive rats. J Hypertens. 2004; 22:1787–1796. [PubMed: 15311108]
19. Arita R, Hata Y, Nakao S, et al. Rho kinase inhibition by fasudil ameliorates diabetes-induced microvascular damage. Diabetes. 2009; 58:215–226. [PubMed: 18840783]
20. Bond JE, Ho TQ, Selim MA, et al. Temporal spatial expression and function of non-muscle myosin II isoforms IIA and IIB in scar remodeling. Lab Invest. 2010
21. Grinnell F. Fibroblast collagen-matrix contraction: growth-factor signalling and mechanical loading. Trends in Cell Biology. 2000; 10:362–365. [PubMed: 10932093]
22. Grinnell F, Petroll WM. Cell Motility and Mechanics in Three-Dimensional Collagen Matrices. Annual Review of Cell and Developmental Biology. 2010; 26:335–361.
23. Friel AM, Hynes PG, Sexton DJ, et al. Expression levels of mRNA for Rho A/Rho kinase and its role in isoprostane-induced vasoconstriction of human placental and maternal vessels. Reprod Sci. 2008; 15:179–188. [PubMed: 18089586]
24. da Silva-Santos JE, Chiao CW, Leite R, et al. The Rho-A/Rho-kinase pathway is up-regulated but remains inhibited by cyclic guanosine monophosphate-dependent mechanisms during endotoxemia in small mesenteric arteries. Crit Care Med. 2009; 37:1716–1723. [PubMed: 19325475]
25. Arturson G. Prostaglandins in human burn-wound secretion. Burns. 1977; 3:112–118.

26. Wang J, Hori K, Ding J, et al. Toll-like receptors expressed by dermal fibroblasts contribute to hypertrophic scarring. J Cell Physiol. 2011; 226:1265–1273. [PubMed: 20945369]
27. Levinson H, Moyer KE, Saggers GC, et al. Calmodulin-myosin light chain kinase inhibition changes fibroblast-populated collagen lattice contraction, cell migration, focal adhesion formation, and wound contraction. Wound Repair and Regeneration. 2004; 12:505–511. [PubMed: 15453832]
28. Rudolph R, Hurn I, Woodward M. Use of colchicine to inhibit wound contraction. Am J Surg. 1981; 141:712–717. [PubMed: 7246862]
29. Teo TC, Naylor IL. Modifications to the rate of wound contraction by allopurinol. Br J Plast Surg. 1995; 48:198–202. [PubMed: 7640851]
30. Tolazzi AR, Tolazzi KD, Garcia M, et al. Influence of leukotriene inhibitor montelukast on wound contraction and cutaneous healing process in rats. Aesthetic Plast Surg. 2009; 33:84–89. [PubMed: 18797959]
31. Fukushima M, Nakamuta M, Kohjima M, et al. Fasudil hydrochloride hydrate, a Rho-kinase (ROCK) inhibitor, suppresses collagen production and enhances collagenase activity in hepatic stellate cells. Liver International. 2005; 25:829–838. [PubMed: 15998434]
32. Ying Z, Yue P, Xu X, et al. Air pollution and cardiac remodeling: a role for RhoA/Rho-kinase. Am J Physiol Heart Circ Physiol. 2009; 296:H1540–H1550. [PubMed: 19286943]
33. Desmouliere A, Geinoz A, Gabbiani F, et al. Transforming growth factor-beta 1 induces alpha-smooth muscle actin expression in granulation tissue myofibroblasts and in quiescent and growing cultured fibroblasts. J Cell Biol. 1993; 122:103–111. [PubMed: 8314838]
34. Abe M, Ho CH, Kamm KE, et al. Different molecular motors mediate platelet-derived growth factor and lysophosphatidic acid-stimulated floating collagen matrix contraction. J Biol Chem. 2003; 278:47707–47712. [PubMed: 14504290]
35. Hirayama K, Hata Y, Noda Y, et al. The involvement of the rho-kinase pathway and its regulation in cytokine-induced collagen gel contraction by hyalocytes. Invest Ophthalmol Vis Sci. 2004; 45:3896–3903. [PubMed: 15505034]
36. Jiang H, Rhee S, Ho CH, et al. Distinguishing fibroblast promigratory and procontractile growth factor environments in 3-D collagen matrices. FASEB J. 2008; 22:2151–2160. [PubMed: 18272655]
37. Parizi M, Howard EW, Tomasek JJ. Regulation of LPA-promoted myofibroblast contraction: role of Rho, myosin light chain kinase, and myosin light chain phosphatase. Exp Cell Res. 2000; 254:210–220. [PubMed: 10640419]
38. Matsui T, Amano M, Yamamoto T, et al. Rho-associated kinase, a novel serine/threonine kinase, as a putative target for small GTP binding protein Rho. EMBO J. 1996; 15:2208–2216. [PubMed: 8641286]
39. Leung T, Manser E, Tan L, et al. A novel serine/threonine kinase binding the Ras-related RhoA GTPase which translocates the kinase to peripheral membranes. J Biol Chem. 1995; 270:29051–29054. [PubMed: 7493923]
40. Ishizaki T, Maekawa M, Fujisawa K, et al. The small GTP-binding protein Rho binds to and activates a 160 kDa Ser/Thr protein kinase homologous to myotonic dystrophy kinase. EMBO J. 1996; 15:1885–1893. [PubMed: 8617235]
41. Tomasek JJ, Vaughan MB, Kropp BP, et al. Contraction of myofibroblasts in granulation tissue is dependent on Rho/Rho kinase/myosin light chain phosphatase activity. Wound Repair and Regeneration. 2006; 14:313–320. [PubMed: 16808810]
42. Desmoulière A, Geinoz A, Gabbiani F, et al. Transforming growth factor-beta 1 induces alpha-smooth muscle actin expression in granulation tissue myofibroblasts and in quiescent and growing cultured fibroblasts. The Journal of Cell Biology. 1993; 122:103–111. [PubMed: 8314838]
43. Abe M, Ho C-H, Kamm KE, et al. Different Molecular Motors Mediate Platelet-derived Growth Factor and Lysophosphatidic Acid-stimulated Floating Collagen Matrix Contraction. Journal of Biological Chemistry. 2003; 278:47707–47712. [PubMed: 14504290]
44. Hirayama K, Hata Y, Noda Y, et al. The Involvement of the Rho-Kinase Pathway and Its Regulation in Cytokine-Induced Collagen Gel Contraction by Hyalocytes. Invest. Ophthalmol. Vis. Sci. 2004; 45:3896–3903. [PubMed: 15505034]

45. Jiang H, Rhee S, Ho C-H, et al. Distinguishing fibroblast promigratory and procontractile growth factor environments in 3-D collagen matrices. FASEB J. 2008; 22:2151–2160. [PubMed: 18272655]

46. Parizi M, Howard EW, Tomasek JJ. Regulation of LPA-Promoted Myofibroblast Contraction: Role of Rho, Myosin Light Chain Kinase, and Myosin Light Chain Phosphatase. Experimental Cell Research. 2000; 254:210–220. [PubMed: 10640419]

47. Totsukawa G, Yamakita Y, Yamashiro S, et al. Distinct Roles of Rock (Rho-Kinase) and Mlck in Spatial Regulation of Mlc Phosphorylation for Assembly of Stress Fibers and Focal Adhesions in 3t3 Fibroblasts. The Journal of Cell Biology. 2000; 150:797–806. [PubMed: 10953004]

48. Castella LF, Buscemi L, Godbout C, et al. A new lock-step mechanism of matrix remodelling based on subcellular contractile events. J Cell Sci. 2010; 123:1751–1760. [PubMed: 20427321]

49. Fukumoto Y, Matoba T, Ito A, et al. Acute vasodilator effects of a Rho-kinase inhibitor, fasudil, in patients with severe pulmonary hypertension. Heart. 2005; 91:391–392. [PubMed: 15710736]

50. Fukui S, Fukumoto Y, Suzuki J, et al. Long-term inhibition of Rho-kinase ameliorates diastolic heart failure in hypertensive rats. J Cardiovasc Pharmacol. 2008; 51:317–326. [PubMed: 18356698]

51. Ishimaru K, Ueno H, Kagitani S, et al. Fasudil attenuates myocardial fibrosis in association with inhibition of monocyte/macrophage infiltration in the heart of DOCA/salt hypertensive rats. J Cardiovasc Pharmacol. 2007; 50:187–194. [PubMed: 17703135]

52. Kanda T, Wakino S, Homma K, et al. Rho-kinase as a molecular target for insulin resistance and hypertension. Faseb J. 2006; 20:169–171. [PubMed: 16267124]

53. Bokoch GM. Regulation of innate immunity by Rho GTPases. Trends in Cell Biology. 2005; 15:163–171. [PubMed: 15752980]

54. Aznar S, Lacal JC. Rho signals to cell growth and apoptosis. Cancer Letters. 2001; 165:1–10. [PubMed: 11248412]

55. Ruperez M, Sanchez-Lopez E, Blanco-Colio LM, et al. The Rho-kinase pathway regulates angiotensin II-induced renal damage. Kidney Int. 2005 Suppl:S39–S45.

56. Heusinger-Ribeiro J, Eberlein M, Wahab NA, et al. Expression of connective tissue growth factor in human renal fibroblasts: regulatory roles of RhoA and cAMP. J Am Soc Nephrol. 2001; 12:1853–1861. [PubMed: 11518778]

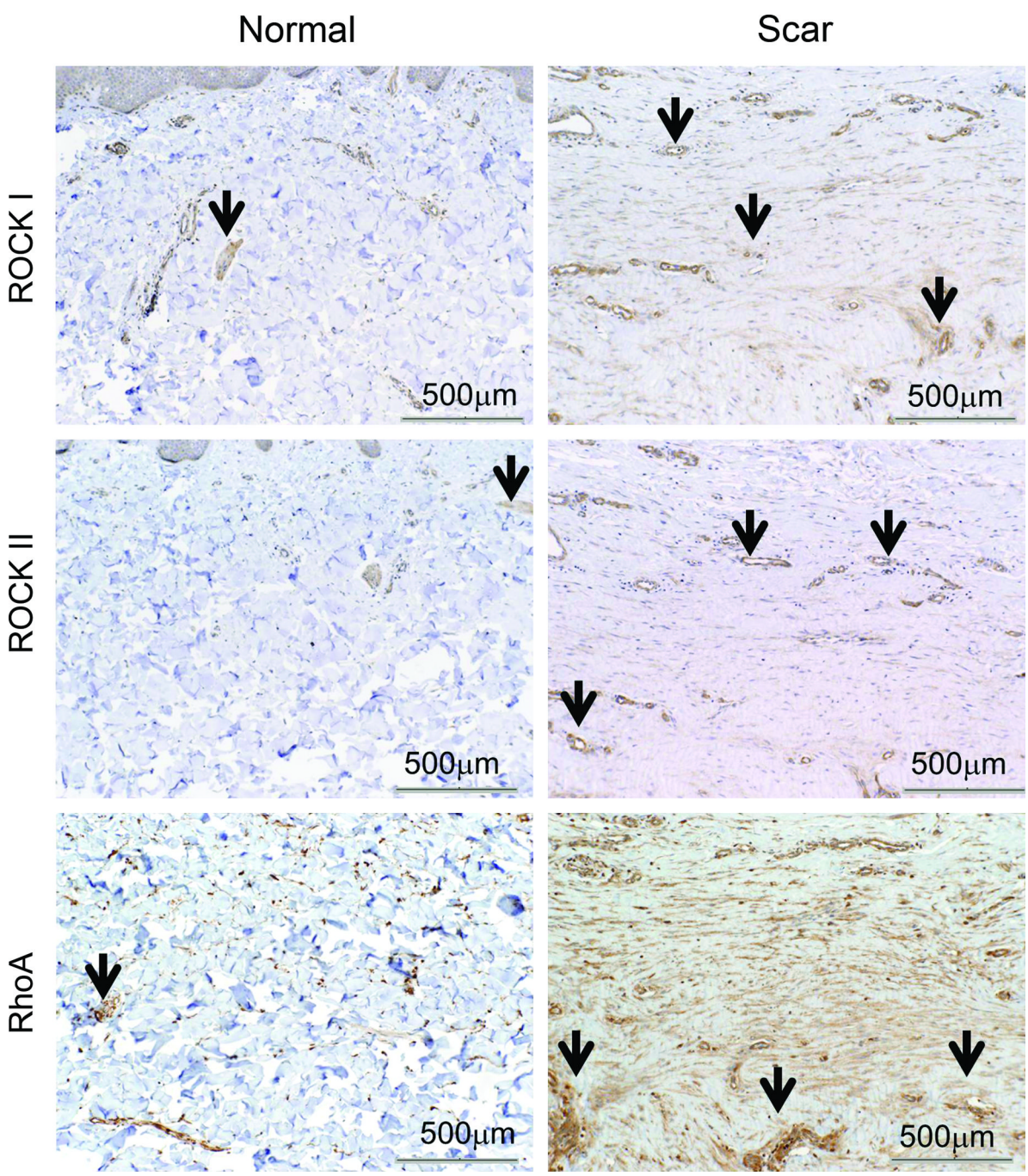

Fig.1.

Representative histological sections of scar tissue (84d post injury in remodeling phase) and normal skin immunostained for RhoA, ROCK I and II. ROCK I and ROCK II are expressed throughout scar tissue but are minimally expressed in normal skin Expression of RhoA is increased in scar tissue compared to normal tissue. Black arrows show positive staining. Postive staining of vessels acting as internal control. 10× magnification, scale bar = 500μm.

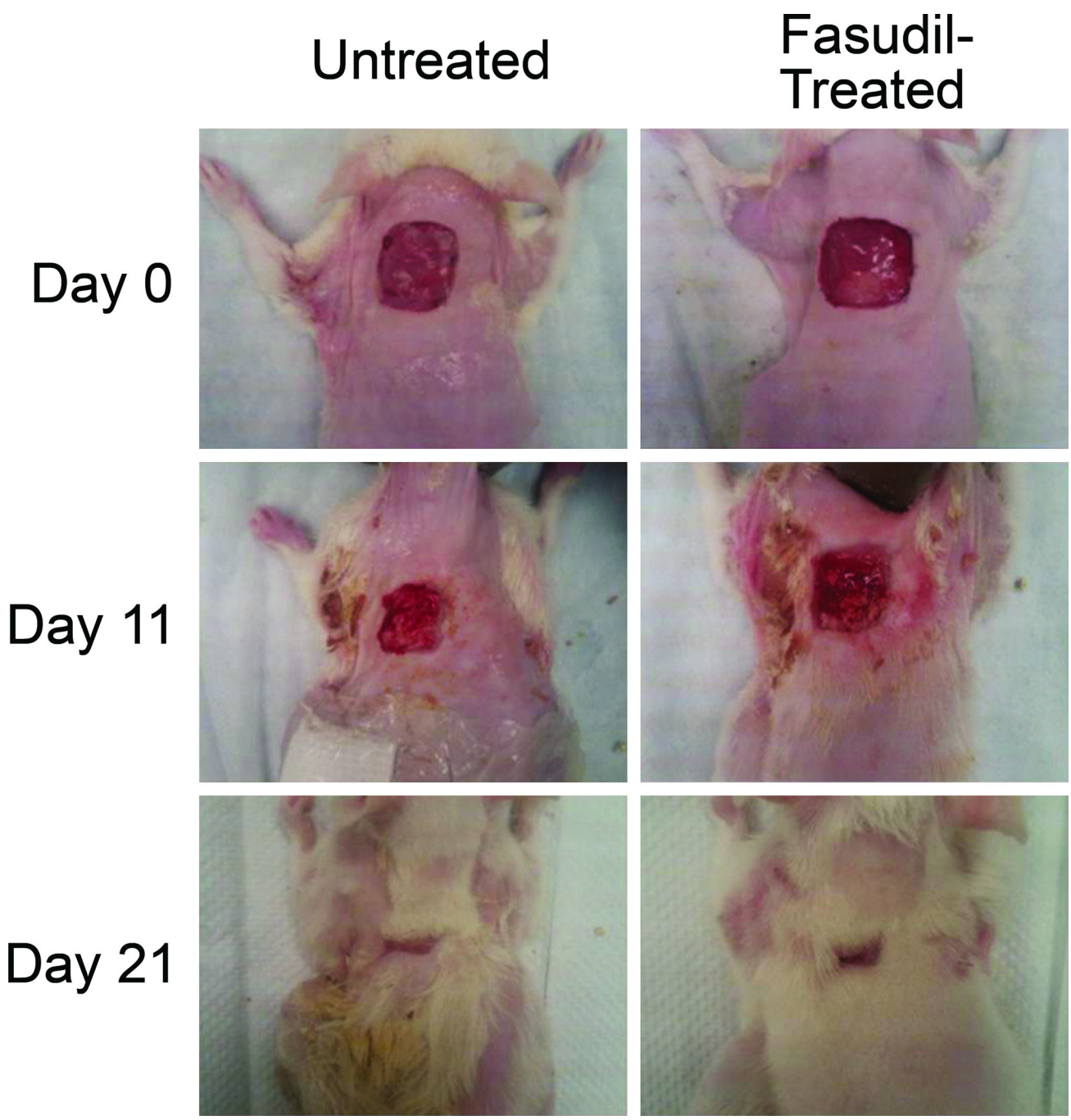

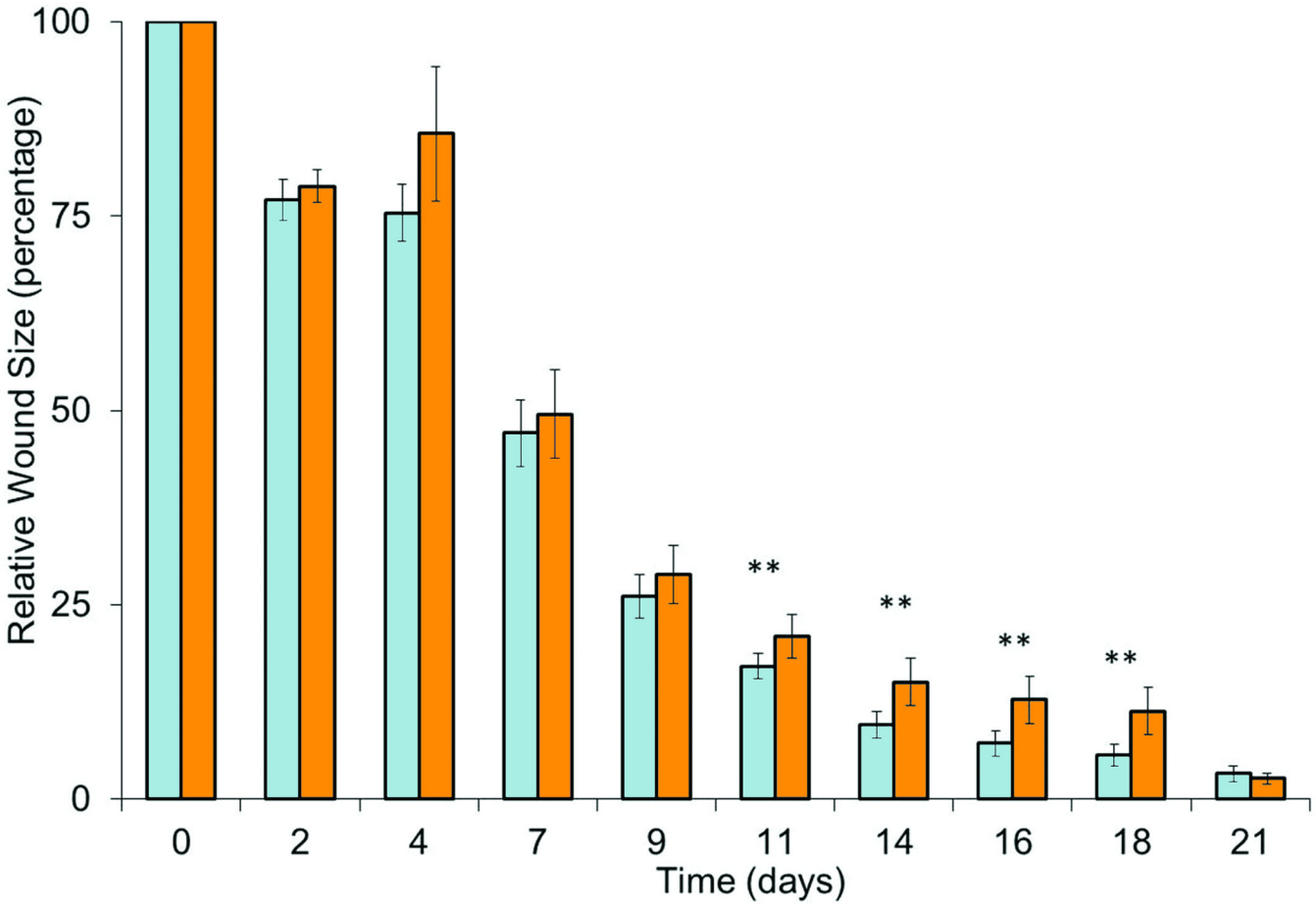

Fig.2.

Contraction of excisional untreated and fasudil-treated wounds. (A) Gross observation of wounds at 0, 11, 21d. (B) The percentage of the wound remaining open relative to the initial wound area at each time point after excision of full thickness wound of 2×2cm of untreated (white) and fasudil-treated (black, 30mg/kg/d) rats. Mean ± SEM; n= 10; $^{**}p < 0.05$.

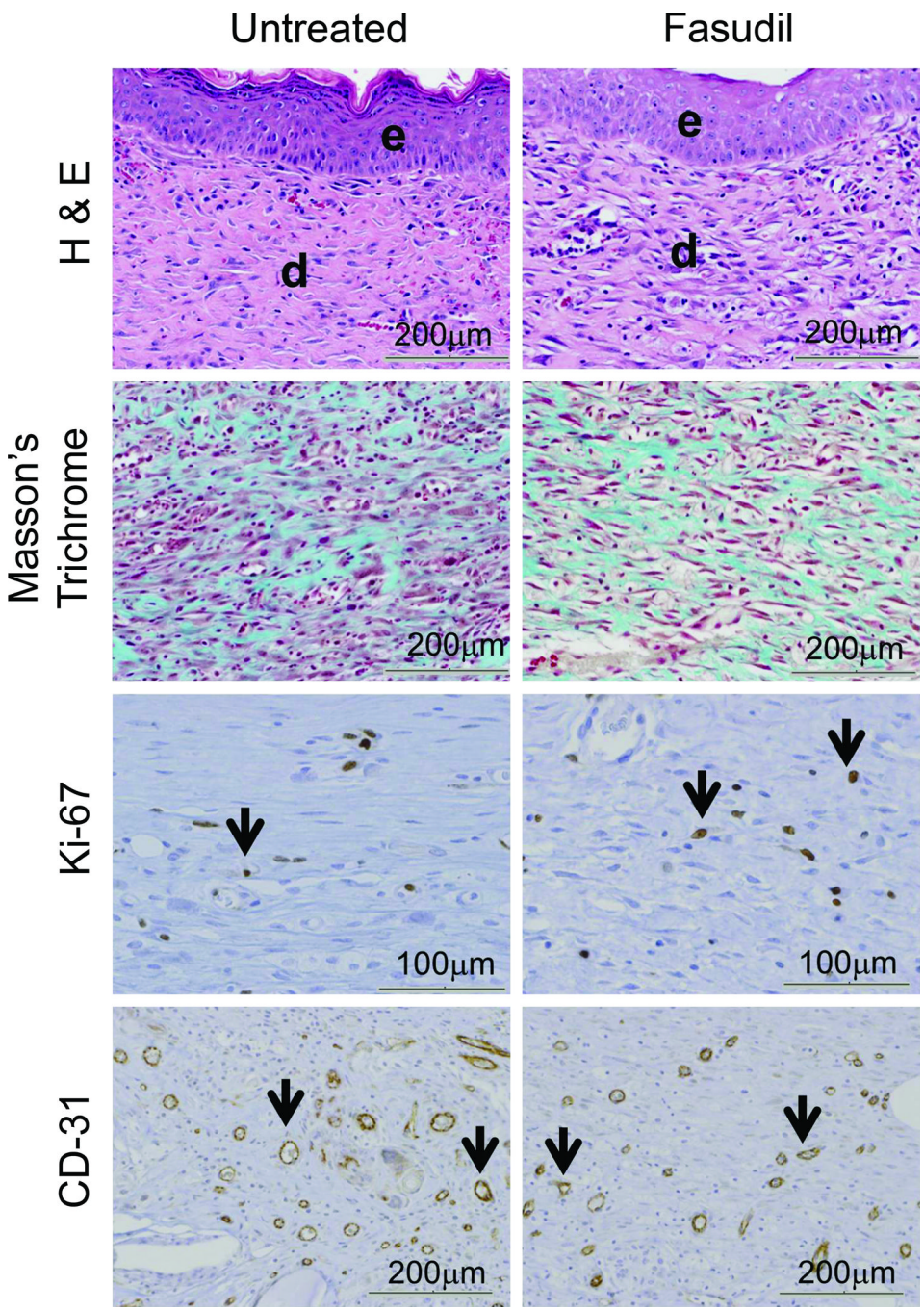

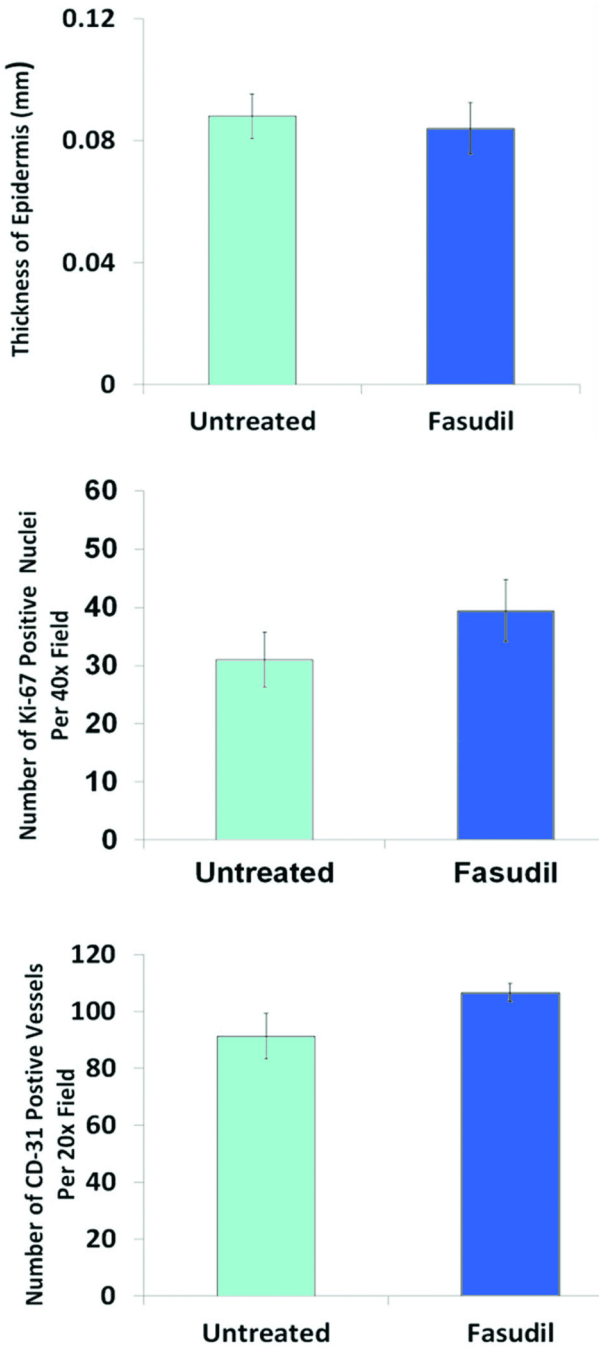

Fig.3.

Histological and Immunohistochemical evaluation of untreated and fasudil-treated wounds. (A) Hematoxylin and eosin showed both groups had high cellularity, including fibroblasts lymphocytes, macrophages (e = epidermis and d = dermis, 20× magnification, scale bar = 200μm). The thickness of the newly formed epidermis was not significantly different between the two groups. Masson`s trichrome stain for collagen revealed a random alignment of collagen fibers in scar tissue. This pattern was similar in both untreated and fasudil treated animals (20× magnification, scale bar = 200μm). Ki-67 staining showed no difference in proliferation between the two groups (black arrows point at Ki-67 positive nuclei). CD-31 staining showed the same degree of neo-vascularization between untreated

and fasudil-treated groups (black arrows point at CD-31 positive vessels). (B) Epithelialization was quantified for each specimen by measuring 5 different epithelium thicknesses. Data shown are mean ± SEM. The number of Ki-67 positive nuclei and CD-31 positive vessels were counted in five 40× and 20× power fields, respectively. Data shown are mean number of Ki-67 positive nuclei per 40× power field ± SEM, n= 5 ($p > 0.05$) and mean number of CD-31 positive vessels per 20× power field ± SEM, n= 5 ($p > 0.05$).

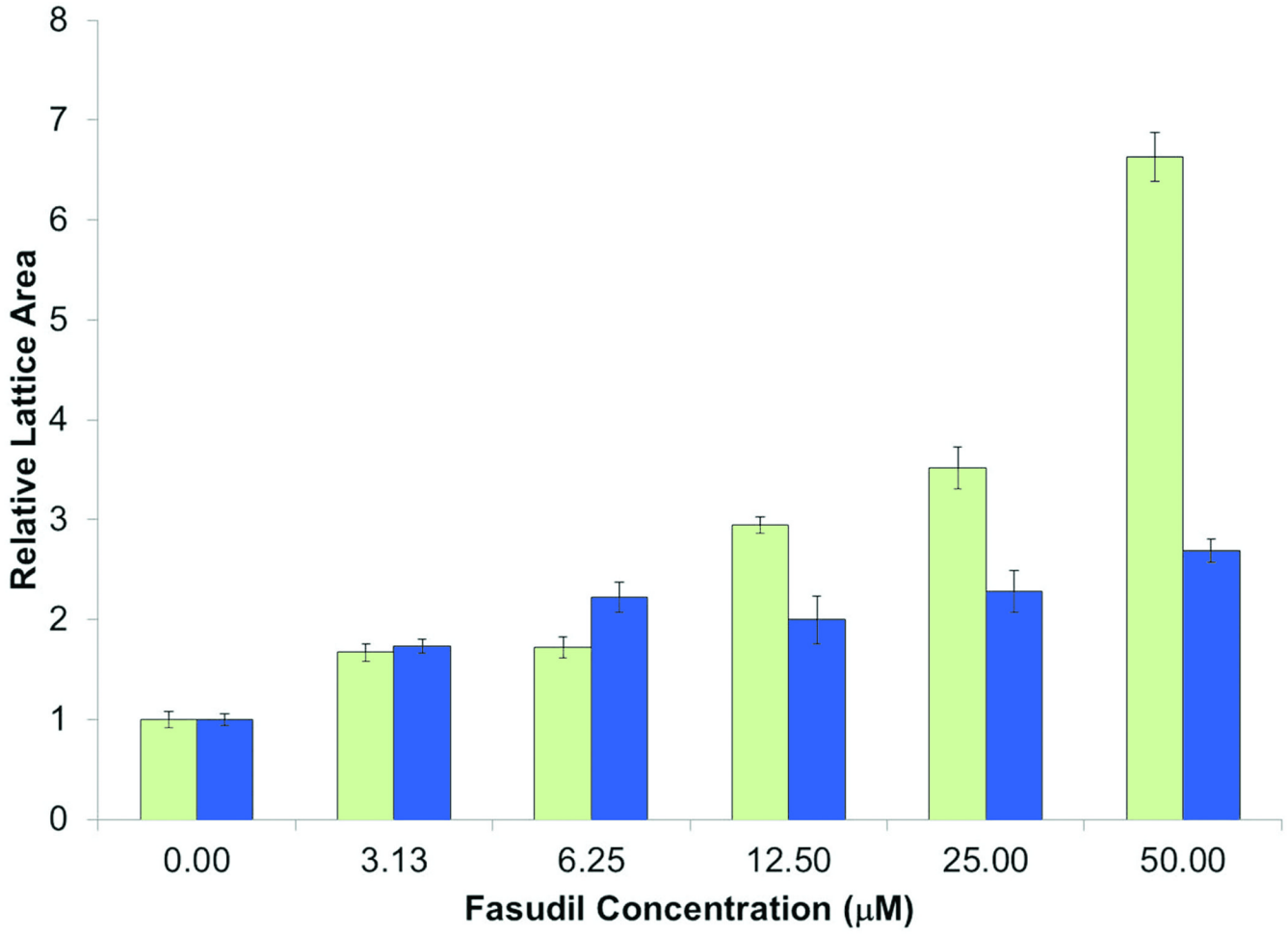

Fig.4.

The effect of fasudil on fibroblast and myofibroblast function. The effect of fasudil on contraction of free-floating or stressed fibroblast populated collagen lattices (FF-FPCL and S-FPCL, respectively). Fibroblast were cultured within 3D collagen lattices, contraction of FPCL was measured by taking images at 18h for FF-FPCL (white) and 5h for S-FPCL (grey) and analysis of the area of the FPLC with ImageJ. Fasudil signfcantly inhibited FPCL contraction at concentrations above 6.25μM ($p \leq 0.05$). Data represents 3 cell lines repeated in triplicate, mean ± SEM, n =9.

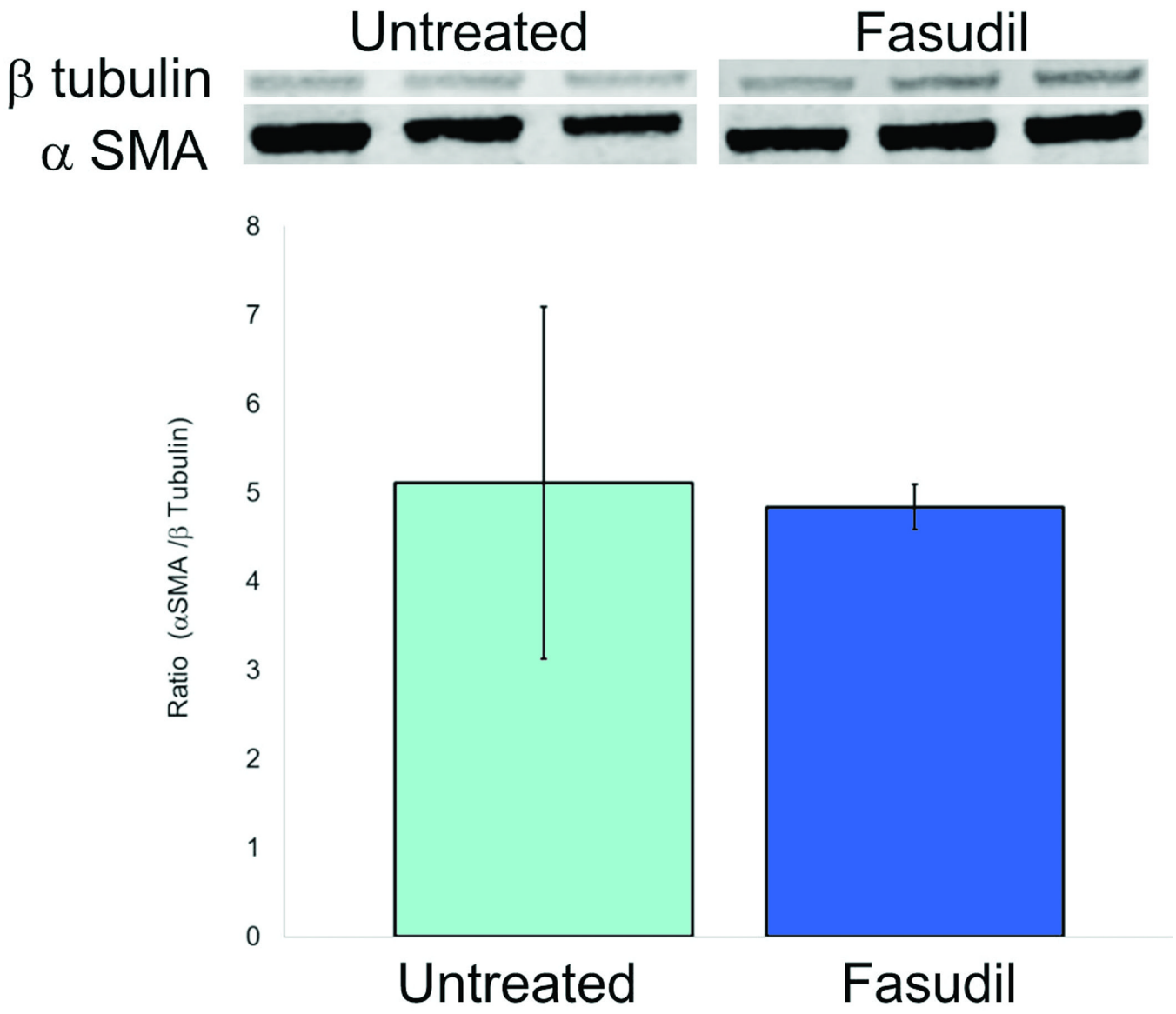

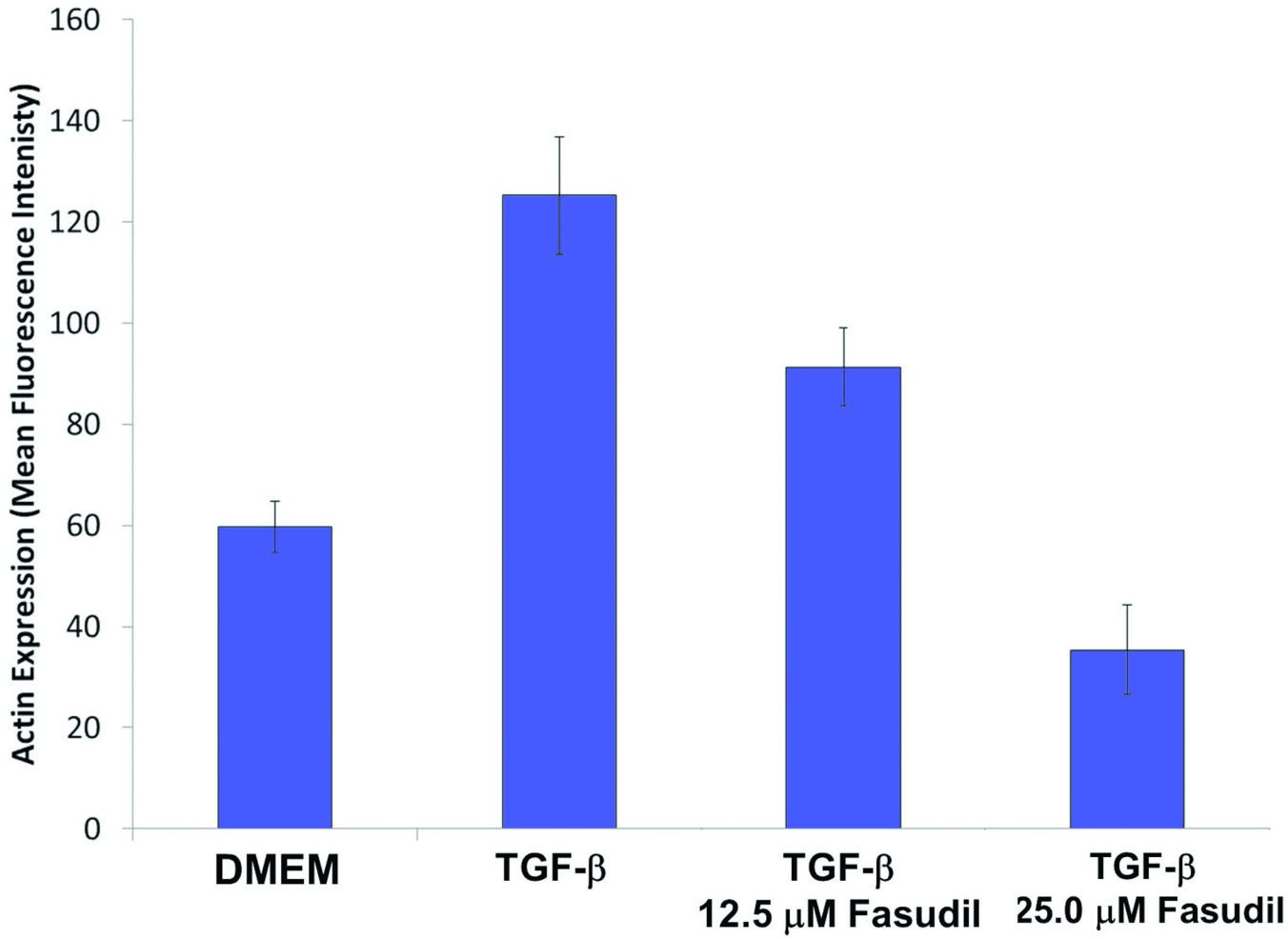

Fig. 5.

The effect of fasudil on alpha smooth muscle actin expression (A) Western blot analysis of 21d tissue for alpha smooth muscle actin expression (αSMA) and beta tubulin (β-tubulin) (B) Primary dermal fibroblasts were incubated with 5ng/ml TGF-β for 4d to differentiate into myofibroblasts in the presence of 12.5μM or 25μM fasudil and αSMA expression measured by intracellular flow cytometry. Data represents mean fluorescence intensity of 3 cell lines, mean ± SEM.

Table 1

Patient Demographic of Selected Scar Samples.

Group		N
Race	Caucasian	32
	Black	1
Gender	Male	17
	Female	16
Age (years)	<50	18
	>50	15
Scar Location	Head	6
	Trunk	12
	Upper extremities	8
	Lower extremities	7
Scar Age	Remodeling:	
	2wks – 6 mos	24
	Male	12
	Female	12
	Post-remodeling	
	>6mos	9
	Male	5
	Female	4